THE JOURNAL OF PHYSICAL CHEMISTRY A

ARTICLE

pubs.acs.org/JPCA

About the Barriers to Reaction of CCl_4 with HFeOH and $FeCl_2$

Bojana Ginovska-Pangovska, Donald M. Camaioni,* and Michel Dupuis

Chemical and Materials Sciences Division, Fundamental and Computational Sciences Directorate, Pacific Northwest National Laboratory, PO Box 999, Richland, Washington 99352, United States

Supporting Information

ABSTRACT: The reactions of zerovalent iron with water and carbon tetrachloride are of interest for environmental remediation of contaminated water and soil. Atom-dropping experiments have shown that the reactions of iron atoms with water and CCl_4 may produce HFeOH and $FeCl_2$, respectively, but these compounds are themselves unreactive toward CCl_4 at the low temperatures under which the atom-dropping experiments were performed. We report a modeling study of these reactions using density functional theory, ab initio Hartree−Fock and couple-cluster theory, and principles of Marcus−Hush theory to characterize the underlying intrinsic barriers and rationalize the experimental results. Electron-correlated CCSD(T) calculations (at B3LYP/TZVP optimized structures) show that the transition state for Cl atom transfer from CCl_4 to HFeOH arises from crossing of electronic states in which the configuration of Fe changes from a quintet high spin state in the Fe^{II} reactant to a sextet high spin state in the Fe^{III} products. The crossing point is 23.8 kcal/mol above a long-range precursor complex that is 2.1 kcal/mol more stable than the separated reactants. The electronic structure changes in these Cl atom transfer reactions involve unpairing of d electrons in Fe^{II} and their recoupling with Cl−C σ bond electrons. These processes can be conveniently described by invoking the self-exchange reactions HFeOH/HFeClOH, $FeCl_2/FeCl_3$, and $CCl_4/^{\bullet}CCl_3$ for which we determined the energy barriers to be 15.5, 13.1, 18.6 kcal/mol, respectively. For the cross reaction $FeCl_2/CCl_4$, we estimated a barrier of 16.6 kcal/mol relative to the separated reactants and 21.1 kcal/mol from the precursor complex. The magnitudes of the reaction barriers are consistent with reports of the absence of products in the atom-dropping experiments.

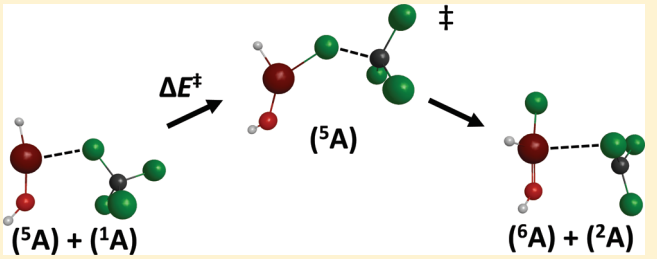

INTRODUCTION

The reaction of zerovalent iron with carbon tetrachloride is of interest for environmental remediation of contaminated water and soil.[1] Thus, Parkinson et al.[2] used a low-temperature "atom-dropping" technique to react Fe atoms with thin films of CCl_4 and water at 35 K. A rich surface chemistry was observed for Fe reacting with neat CCl_4.[2,3] These authors identified products including C_2Cl_4, C_2Cl_6, $OCCl_2$, CO, $FeCl_2$, and $FeCl_3$. In conjunction with this work, we calculated reactions pathways for these reactions that we discovered involved formation of very stable intermediates containing Fe−C bonds.[4] Such compounds had been identified in matrix isolation experiments.[5] When Fe atoms were reacted with neat water (ice) films, Parkinson et al.[6] observed that HFeOH was produced. HFeOH was thermally stable up to ∼150 K, the temperature at which water sublimes from the surface. It also appeared that HFeOH reacted with oxide ions of the supporting FeO(111) surface. In experiments[2] that dropped Fe atoms onto bilayers of water and CCl_4 with water on top, HFeOH would form before encountering CCl_4. No evidence was detected of HFeOH reacting with CCl_4. Thus, it appeared that the HFeOH/CCl_4 reaction is too slow to compete with thermal desorption of CCl_4. Complementing this result, Parkinson et al.[3] had shown that $FeCl_2$ is unreactive with CCl_4, and they estimated that the reaction of $FeCl_2$ with CCl_4 must have a reaction barrier > 12 kcal/mol. We investigated the title reactions to gain insight into the absence of reactivity of HFeOH and $FeCl_2$ toward CCl_4 in the atom-dropping experiments.

We note that the reactivity of $FeCl_2$ with CCl_4 and $RCCl_3$ has been studied in solution.[7−9] Bimolecular rate constants are on the order of 10^{-4} M^{-1} s^{-1} at room temperature. Cornia et al.[9] determined an activation barrier of ∼14 kcal/mol for α,α,α-trichlorotoluene in acetonitrile. Before the work presented here, Mebel and Hwang[10] and Zhang and co-workers[11] modeled the reaction of atomic iron with H_2O, while Gutsev et al.[12] characterized structures derived from water interacting with iron clusters. In both studies, stable HFeOH structures with Fe inserted into one of the OH bonds of H_2O were reported. We obtained similar structures in our study. Mebel and Hwang[10] calculated a high barrier, ∼33 kcal/mol at the CCSD(T) level of theory, for the reaction of Fe^0 with a single H_2O molecule in the gas phase. However, in the atom-dropping experiments of Parkinson et al., HFeOH was observed in reactions of atomic Fe with water layers at 35 K. We suggest that this observation shows that the reaction of Fe^0 with water in the condensed phase has a very low barrier due to the involvement of multiple water molecules. This interpretation of the formation of HFeOH

Received: March 1, 2011
Revised: June 25, 2011
Published: June 27, 2011

involving several water molecules in the condensed phase at low temperature would require computational support, which however is not essential to the present purpose and investigation.

Here, we report a modeling study to characterize the barriers of Cl atom transfer reactions 1 and 2 using electronic structure theory.

$$HFeOH + CCl_4 \rightarrow HFeClOH + {}^{\bullet}CCl_3 \quad (1)$$

$$FeCl_2 + CCl_4 \rightarrow FeCl_3 + {}^{\bullet}CCl_3 \quad (2)$$

A difficulty encountered in modeling these systems is that the electronic structure changes along the reaction path due to a change in the oxidation state of Fe. The transition states (TSs) arise from a crossing of electronic states in which the configuration of Fe changes from a quintet high spin state in the Fe^{II} reactant to a sextet high spin state in the Fe^{III} products such that the wave function exhibits multireference character. We succeeded in calculating the states that cross in reaction 1 and estimated the barrier from the crossing point. We were not successful in determining the wave functions and structures near the TS for reaction 2. Therefore, we resorted to estimating the barriers of both reactions 1 and 2 using principles of Marcus–Hush theory,[13−15] and for this purpose, we characterized the barriers for the identity reactions 3−5.

$$ {}^{\bullet}CCl_3 + CCl_4 \rightarrow CCl_4 + {}^{\bullet}CCl_3 \quad (3)$$

$$FeCl_2 + FeCl_3 \rightarrow FeCl_3 + FeCl_2 \quad (4)$$

$$HFeOH + HFeClOH \rightarrow HFeClOH + HFeOH \quad (5)$$

In the Marcus–Hush theory, the activation free energy $\Delta G^{\ddagger}$ is given by eq 6

$$\Delta G^{\ddagger} = W_R + \Delta G_0^{\ddagger}\left(1 + \frac{\Delta G^{\circ} - W_R + W_P}{4\Delta G_0^{\ddagger}}\right) \quad (6)$$

where $\Delta G_0^{\ddagger}$ is the intrinsic barrier of the reaction, ΔG° is the free energy of the reaction, and W_R and W_P are the free energies for forming the encounter complexes from the separated reactants and products, respectively. The intrinsic barrier $\Delta G_0^{\ddagger}$ corresponds to the barrier of the reaction in the absence of a driving force, that is, when $(\Delta G^{\circ} - W_R + W_P)$ is hypothetically equal to 0. In theory, $\Delta G_0^{\ddagger}$ is estimated by the cross relationship that equates the intrinsic barrier of a reaction, for example, reaction 2, to the average of the intrinsic barriers of the constituent identity reactions 3 and 4 when considering reaction 2. This approach of extracting a cross-reaction barrier from the intrinsic barriers of identity reactions has been extensively used for electron transfer reactions, proton-coupled electron transfer,[16] and hydrogen transfer,[17−19] as well as halogen atom transfer reactions between two metal centers.[20,21] We note that the Cl atom transfer between the two metal centers as in reactions 4 and 5 may also be described as an innersphere electron transfer coupled with the transfer of a bridging chloride ligand with a presumably weak donor–acceptor coupling owing to the separation of the donor and acceptor sites, and as such, it can be subjected to the Marcus–Hush treatment. Finally, because we are interested in the low-temperature regime, we used zero-point corrected energies in place of free energy.

The wave functions for the structures involved in the identity reactions 4 and 5 exhibit multireference character due to the change in electronic/oxidation state of Fe along the reaction path. Therefore, we estimated the barriers by determining the crossing point between the two quasi-diabatic energy curves that underlie the barriers by gradually transferring a chlorine atom between the Fe centers while maintaining the character of the wave function from one step to the next. Within the Marcus–Hush electron transfer model, two diabatic states A and B (see Figure 1) combine linearly to give rise to two adiabatic states E_- (ground state) and E_+ (excited state). The adiabatic barrier is approximated by subtracting from the crossing point energy half of the energy difference between the ground and excited states at the crossing point. The difference at the crossing point may be calculated from the transition matrix element $H_{AB} = (\Psi_A|H|\Psi_B)$ determined directly from the quasi-diabatic states[22] or using the generalized Mulliken–Hush (GMH) approach that makes use of E_-, E_+, and the transition dipole matrix element of the adiabatic states.[22,23] Alternately, the energy splitting $(E_+ - E_-)$ may be calculated directly at the CCSD(T)[23,24] level of theory using the equation-of-motion formalism EOM-CCSD(T).[25] In reactions such as 4 and 5 that have strong nonadiabatic character reflected in a small energy difference between the ground and excited states, the barrier is sharp, and the reaction curves follow closely the quasi-diabatic curves, justifying the use of the curve-crossing method to estimate barriers.

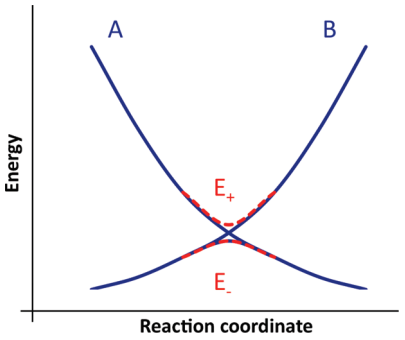

Figure 1. Curve-crossing diagram showing the relationship between two diabatic states (A and B) and the two adiabatic states (E_- and E_+) resulting from the mixing of A and B.

METHODS

The calculations were performed using the Gaussian98,[26] Gaussian-09,[27] and NWChem 5.1.1[28] electronic structure codes. All structures reported in this study were optimized using either the Hartree–Fock (HF) or density functional[29,30] (DFT) levels of theory. Single-point energies of the optimized structures were calculated at the level of coupled-cluster theory with singles and doubles excitations and perturbative treatment of triple excitations (CCSD(T)). For the open-shell systems, we used the spin-unrestricted formulation of the theory (U-CCSD(T)). For HF optimizations, we used the 6-31G* basis set[31] for C, Cl, O, and H and Ahlrichs VTZ basis set[32] for Fe. For DFT calculations, we used the B3LYP functional[33] with the Ahlrichs TZV basis set[34] supplemented with polarization functions (d functions on C and Cl with exponents of 0.8 and 0.65, respectively, and p functions on Fe with an exponent of 0.135) and the Ahlrichs VTZ for hydrogen. In our previous work,[4] we assessed the performance of this level of theory and found it to yield energetics and structures of semiquantitative accuracy. The single-determinant spin-unrestricted Hartree–Fock (UHF) and Kohn–Sham

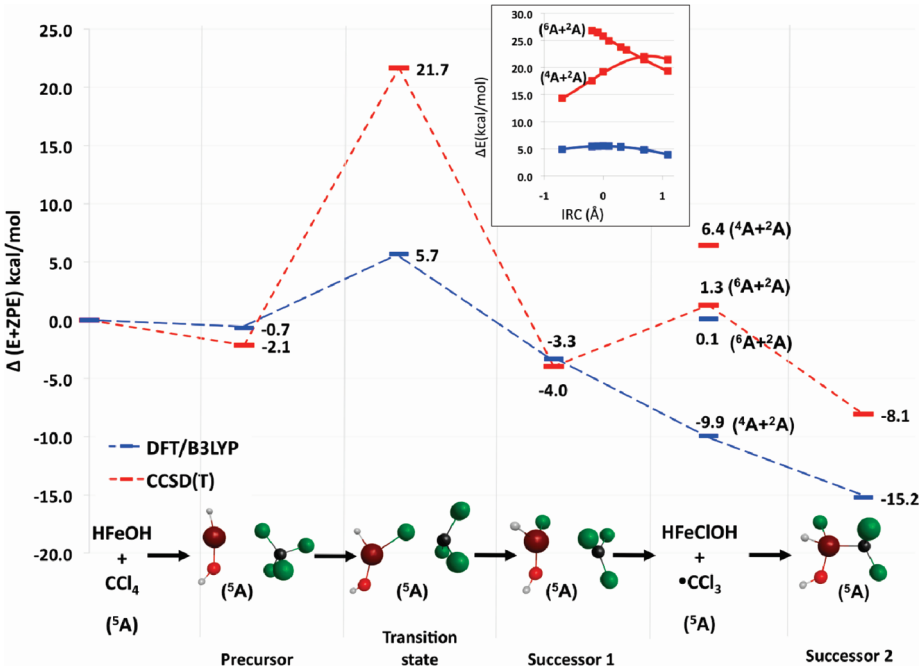

Figure 2. Energy diagram for the reaction of Cl abstraction from CCl_4 by HFeOH on the quintet potential energy surface. The geometries are optimized at the DFT(B3LYP) level of theory with Ahlrichs TZV basis set (VTZ for H atoms). The inset shows the electronic state crossing on the CCSD(T) quintet potential energy surface in the region near the transition state (~0.5 Å along the IRC toward the products). The CCSD(T) energy at the crossing point is 21.7 kcal/mol above the energy of the separated rectants, whereas the DFT barrier of 5.7 kcal/mol is at the DFT transition state. In the inset, the DFT TS structure is at 0 Å.

(UKS) wave functions were tested for stability in all cases.[35,36] Frequency calculations were carried out for all of the structures, and the unscaled frequencies were used to calculate zero-point corrections. For reactions 1 and 3, TS structures were calculated (as first-order saddle points on the DFT potential energy surface (PES) with one imaginary frequency), and the barriers were calculated as the energy difference between the reactants and the TS. For reaction 2, a saddle point could not be determined at either the HF or DFT levels of theory. Therefore, we resorted to getting a numerical estimate of the barriers using Marcus−Hush theory. For the self-exchange reactions 4 and 5, the adiabatic barriers for Cl atom transfer were extracted by determining a quasi-diabatic crossing point and estimating the electronic coupling between the two quasi-diabatic states. The electronic coupling was estimated as half of the energy difference between the ground and exited electronic states calculated with EOM-CCSD(T) theory, as discussed above.

RESULTS AND DISCUSION

We present below the characterization of reactions 1−5. We report the calculations of the reaction energies and the energies for forming encounter complexes, as well as the calculation of the adiabatic barriers for reactions 1 and 3. We also discuss the calculation of barriers for reactions 1, 4, and 5 from the crossing points of the diabatic curves. We then use the data to estimate the barriers of reactions 1 and 2 according to Marcus−Hush theory. We end with a general discussion of the findings.

Reaction 1 of HFeOH with CCl_4. For reaction 1, we determined the shape of the potential energy surface by optimizing the stationary points (reactants, products, precusor and successor complexes, and TS) on the PES and characterizing the intrinsic reaction coordinate (IRC) pathway near the TS, all of this at the DFT level of theory. We then carried out single-point energy calculations at the CCSD(T) level of theory. On the reactant side of the IRC, the electronic state of the system corresponds to a $Fe^{II}(d^6)$ state (HFeOH). On the product side of the IRC, the electronic state of the system corresponds to a $Fe^{III}(d^5)$ state (HFeClOH). The adiabatic TS arises from an avoided crossing between these two states. At the CCSD(T) level of theory with the HF wave function as a reference, we observed that the CCSD(T) expansion maintained the character of the reactant state coming up the IRC from the reactant side and of the product state coming up from the product side, and in both cases, the character was maintained going across the DFT(B3LYP) transition state. In essence, the CCSD(T) calculations yielded quasi-diabiatic reactant and product states, and we observed the crossing of these states along the DFT reaction pathway. The crossing curves are shown in the inset of Figure 2. We used the CCSD(T) energy at the crossing point to extract the reaction barrier.

The energy diagram depicting the stability of the various species on the quintet spin potential energy surface is presented in Figure 2. Energies of the various species and complete structural data for this reaction and all other reactions in this paper are provided in the Supporting Information. Previous work[10,12] as well as our own calculations showed that the most stable state for HFeOH (−58.9 kcal/mol relative to Fe + H_2O) has a quintet spin state with an $Fe^{II}(d^6)$ configuration. The HFeOH structure is planar with a nearly colinear H−Fe−O conformation and a Fe−O−H angle of 144.2°. The oxidation state of Fe in the HFeClOH product of reaction 2 is formally $Fe^{III}(d^5)$. As such, there exist sextet, quartet, and doublet spin states for this electronic structure. The DFT sextet state structure has a planar geometry with the ligands around the Fe atom in a nearly trigonal conformation. The DFT level of theory gives the quartet state

dx.doi.org/10.1021/jp2019928 |J. Phys. Chem. A 2011, 115, 8713–8720

~10.0 kcal/mol below the sextet state. The CCSD(T) level of theory, on the other hand, gives the sextet state ~5.1 kcal/mol more stable than the quartet state. This finding is consistent with high-level electronic structure calculations of Fe^{III} species with weak ligands, such as $FeCl_3$, that show the high spin (d^5) state to be lowest in energy.[37] In Tables S1 and S3 of the Supporting Information, we show DFT and CCSD(T) energies for the stable structures along the reaction path. The calculated and expected S^2 values for all of the structures are also reported in order to show the spin contamination. At the DFT level, no significant spin contamination was observed. In what follws, we give a description of the structures of the precursor, TS, and successor complexes.

Precursor Complex in Reaction 1. The initial step in the reaction with HFeOH (^{5}A) is the formation of a weakly bound H(HO)Fe···$ClCCl_3$ precursor complex, with r_{Fe-Cl} = 2.91 Å, r_{C-Cl} = 1.83 Å, and a H−Fe−O angle of 168.2°. The smaller H−Fe−O angle is suggestive of a site on Fe opening for interaction with one of the Cl atoms from CCl_4. The precursor complex is 2.1 kcal/mol lower in energy than the separated reactants at the CCSD(T)//DFT level of theory. At low temperatures and in the condensed phase (i.e., the conditions of the atom-dropping experiment), the existence of the precursor complex is an important factor that effectively raises the barrier to reaction. In this context, the DFT level of theory underestimates the well depth for the precursor complex as well as the activation barrier (see Figure 2). This is in line with established precedents that the B3LYP functional in DFT underestimates reaction barriers and stabilization energies associated with long-range dispersive interactions.[38−40] The present results are further illustration of these B3LYP deficiencies.

TS Complex in Reaction 1. At the DFT level of theory, the reaction proceeds via a transition state where the distances from C and Fe to the transferring Cl atom are 2.20 and 2.32 Å, respectively. The Fe−Cl−C angle is found to be 134.5°. The HFeClOH moiety is nearly planar with a H−Fe−Cl angle of 90.6°, significantly smaller than that in the precursor complex. At the CCSD(T)//DFT level of theory, this complex is 18.9 kcal/mol higher in energy than the separated reactants (HFeOH + CCl_4) and 21.0 kcal/mol higher than the precursor complex. Furthermore, at the CCSD(T) level of theory, a low-lying excited state for the TS structure was calculated to be ~6.6 kcal/mol higher in energy. CCSD(T) calculations of points along the DFT IRC near the DFT transition state yielded two quintet states close in energy with a curve crossing past the TS on the CCSD(T) potential energy surface (inset Figure 2). The excited state at the DFT TS structure becomes the lowest-energy state beyond the CCSD(T) crossing. The crossing point is ~23.8 kcal/mol above the energy of the precursor complex. That the CCSD(T) crossing point is later than the DFT transition state on the DFT reaction path is in accord with Hammond's postulate[41] as the product state is less stable on the CCSD(T) surface than that on the DFT surface. At the crossing point, the C−Cl bond is 2.27 Å, and the Fe−Cl bond is 2.30 Å. We note that the UHF ground-state wave function used as the reference in the CCSD(T) calculations showed spin contamination (S^2 = 6.37, in contrast to the theoretical value S^2 = 6.0) at the TS. However, the CCSD(T) theory is known to recover in large part the error from the spin contamination.[42]

A natural bond orbital (NBO) population analysis[43] of the SCF density for the DFT ground state and for the UHF ground and excited states (the reference states for the CCSD(T) calculations) at selected points along the DFT IRC provided insight into the significant differences between the DFT and CCSD(T) potential energy surfaces. At the DFT transition state (IRC coordinate = 0.0 Å), an electronic configuration for the DFT wave function was obtained with 4.87 α electrons and 1.44 β electrons in the 3d orbitals of Fe. This configuration is similar to that of the $Fe^{II}(d^6)$ precursor complex with one doubly occupied d orbital on Fe. The same electronic configuration was maintained along the DFT IRC, leading to the HFeClOH (^{4}A) + $^{\bullet}CCl_3$ (^{2}A) product ground state. In contrast, the UHF wave function at the DFT TS geometry showed 4.99 α and 0.39 β electrons in the 3d orbitals on Fe, indicative of all of the 3d orbitals on Fe^{III} being singly occupied. This state correlates with the most stable HFeClOH (^{6}A) + $^{\bullet}CCl_3$ (^{2}A) product state on the quintet surface.

Successor Complexes in Reaction 1. We located two successor complexes on the product side of reaction 1. As shown in Figure 2, these complexes both contain the HFeClOH and $^{\bullet}CCl_3$ fragments, but they differ in that the fragments in successor 1 are weakly bound by long-range interaction predominantly between the Fe atom and one of the Cl atoms of $^{\bullet}CCl_3$, whereas the fragments in successor 2 are bound via a Fe−C bond. Successor 1 exists in two different spin states, quintet and septet, on two potential energy surfaces of corresponding spin. The two spin states originate from the coupling of the sextet spin of the ground state of HFeClOH (^{6}A) with the doublet spin of the $^{\bullet}CCl_3$ radical, resulting in quintet and septet spin states. In successor 1, the Fe center interacts with one Cl atom of the $^{\bullet}CCl_3$ radical through a long bond to the halogen atom. In the quintet structure, this bond is 3.34 Å, while it is 2.77 Å in the septet structure, implying a stronger interaction between $^{\bullet}CCl_3$ and H(HO)FeCl in the septet state. Except for the Fe−C distance, the quintet and septet structures have other similar bond lengths. The Fe−Cl−C angles differ by 12, 90.6, and 102.5° for the quintet and septet structures, respectively. The products of the reaction of HFeOH with CCl_4 are HFeClOH and a $^{\bullet}CCl_3$ radical, with the HFeClOH molecule in its sextet ground state with $Fe^{III}(d^5)$ character. The separated products are +1.3 kcal/mol higher in energy than the separated reactants. The endothermicity for this reaction is consistent with the barrier for Cl atom transfer being high.

Successor 2 has an Fe−C bond. It exists both on quintet spin and triplet spin energy surfaces. In the quintet state, the Fe−C bond is 2.1 Å, and the C−Cl bonds are nearly eclipsed with the Fe−H, Fe−Cl, and Fe−O bonds. There is also an Fe···Cl long-range interaction between Fe and a second Cl atom (2.57 Å). This complex is 8.1 kcal/mol more stable than the separated reactants HFeOH + CCl_4. In the triplet state, the Fe−C bond is slightly shorter, 1.99 Å, and the $^{\bullet}CCl_3$ moiety is in a staggered conformation with respect to the O, H, and Cl atoms linked to Fe. The triplet structure exhibits a shorter Fe−O bond (1.73 Å) than the quintet structure and is 4.5 kcal/mol lower in energy than the separated reactants. Successor 2 can be formed by recombination of the dissociated fragments or directly from successor 1.

Reaction of $FeCl_2$ with CCl_4. For reaction 2, we encountered difficulties while attempting to characterize the potential energy surface due to a change in the electronic state and multirefrence character of the wave function near the transition state. Therefore, we resorted to estimating the barrier by determining the intrinsic barriers for the identity (self-exchange) reactions 3 and 4. We succeeded in finding encounter complexes for the reactants

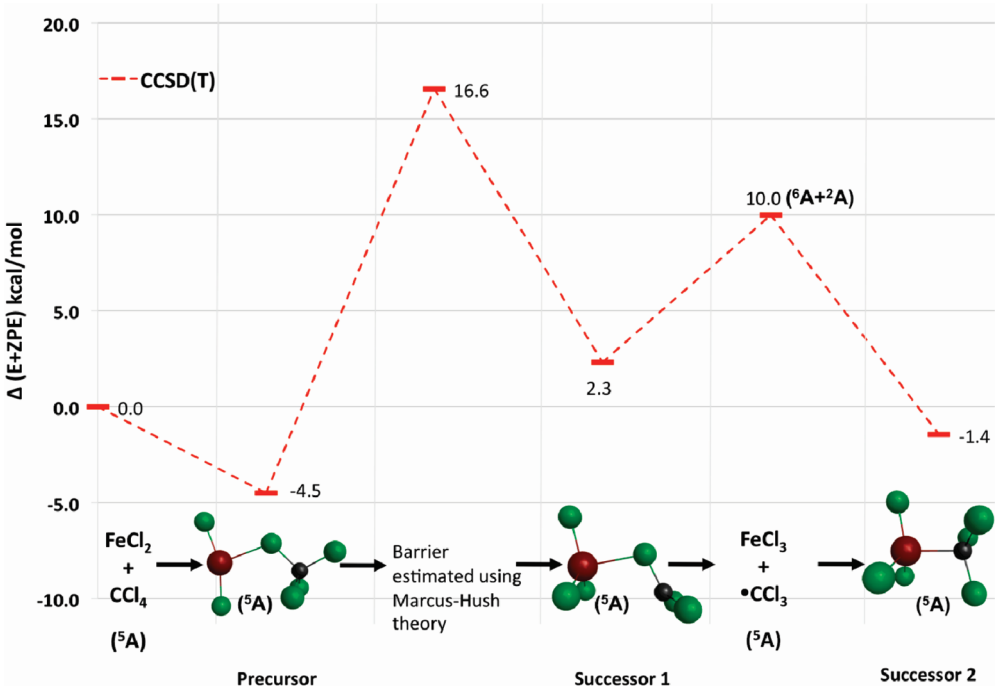

Figure 3. Energy diagram for the reaction of Cl abstraction from CCl_4 by $FeCl_2$ on the quintet potential energy surface. The geometries are optimized at the CCSD(T)/(Ahlrichs TZV+p, VTZ+p for H)//DFT(B3LYP)/(Ahlrichs TZV+p, VTZ+p for H). The barrier was estimated from the intrinsic barriers of the self-exchange reactions using eq 7.

and products, as shown in Figure 3. These structures were optimized at the DFT level of theory, and their energies were calculated with the CCSD(T) theory. In both calculations, the Ahlrichs TZV+p basis set was used. The reaction energy from separated reactants to separated products is +10 kcal/mol. The precursor complex is 4.5 kcal/mol more stable than the separated reactants, and the successor complex is 7.7 kcal/mol more stable than the separated products (see Figure 3). In the precursor complex, the $FeCl_2$ fragment is noticeably distorted from the linear structure of an isolated molecule, with a Cl−Fe−Cl angle of 160°. The transferring Cl atom bridges the Fe and C centers at a Fe−Cl−C angle of 116.7°. The C−Cl and Cl−Fe distances are 1.85 and 2.77 Å, respectively. In the successor complex, the $^{\bullet}CCl_3$ moiety interacts with the $FeCl_3$ moiety by forming a stretched Fe−Cl bond of 2.26 Å. This structure has a quintet spin, with a sextet spin $FeCl_3$ species and a doublet $^{\bullet}CCl_3$ radical. Similar to the reaction sequence for HFeOH with CCl_4 shown in Figure 2, we calculated a second successor complex Cl_3FeCCl_3 on the quintet surface with an Fe−C bond. The structure has C_{3v} symmetry with bond lengths r_{Fe-C} = 2.33 Å, r_{Fe-Cl} = 2.17 Å, and r_{C-Cl} = 1.74 Å and is 1.4 kcal/mol more stable than the reactants.

Self-Exchange Reaction $^{\bullet}CCl_3$ + CCl_4. For this reaction, we optimized the geometries at the DFT (B3LYP) level of theory. We then calculated the energies for these structures at the CCSD(T) level of theory. In the long-range complex, the CCl_4 fragment has C−Cl bonds of 1.79 Å, and in $^{\bullet}CCl_3$, the C−Cl bonds are 1.74 Å. The two fragments are separated by a distance of 3.87 Å measured from the carbon of CCl_3 to the nearest Cl of CCl_4. The Cl−C−Cl angle is 180°. In the TS structure (D_{3d} symmetry), the distance from C to the transferring Cl is 2.19 Å, significantly longer than the other C−Cl bonds (1.76 Å). The CCSD(T) barrier with DFT zero-point correction for this reaction is +19.4 kcal/mol relative to the precursor complex and +18.6 kcal/mol relative to the separated reactants. The C−Cl bond dissociation energy in CCl_4 was calculated to be 62.0 kcal/mol.

Cl Self-Exchange Reactions 4 $FeCl_2$ + $FeCl_3$ and 5 HFeOH + HFeClOH. For the self-exchange reactions 4 and 5, we also had difficulties in optimizing structures that we could characterize as adiabatic TSs for Cl atom transfer due to the change in electronic state from ($d^6 \times d^5$) to ($d^5 \times d^6$). Instead, we extracted the adiabatic barrier by determining the quasi-diabatic crossing point for Cl atom transfer and calculating the electronic coupling between the two quasi-diabatic states. A discussion of the nature of the quasi-diabatic state is given below. Finally, structures of the encounter complexes for Cl transfer in reactions 4 and 5 were optimized with C_{2v} and C_s symmetry, respectively. In the absence of this constraint, the systems adopted four-member ring structures with the Fe atoms bridged by two Cl atoms in reaction 4 and by one Cl atom and one O atom in reaction 5. The bridged structures result from the increased stabilization provided by a second Fe−X bond (X = Cl, O) in addition to the Fe−Cl bond. We deem such structures to be less relevant when characterizing the self-exchange reactions that underlie a Marcus−Hush treatment for determining the barriers in reactions 1 and 2, where only one Fe−Cl bond is broken and formed. The minimum-energy structures in reactions 4 and 5 were optimized using the UHF level of theory and Ahlrichs VTZ basis set for Fe and the 6-31G* basis set for Cl. Single-point energy calculations were carried out at the CCSD(T) level of theory with the Ahlrichs TZV+p basis set.

$FeCl_2$ + $FeCl_3$ Self-Exchange Reaction 4. The precursor complex was optimized in C_{2v} symmetry as a high spin planar structure with a ($d^6 \times d^5$) electronic state. The system exhibited a stable, weakly bound minimum-energy structure $Cl_2Fe\cdots Cl-FeCl_2$ with an Fe···Cl bond distance of 2.97 Å compared

dx.doi.org/10.1021/jp2019928 |J. Phys. Chem. A 2011, 115, 8713–8720

Table 1. Energetics (E + ZPE) in kcal/mol for Identity Reactions and Cross Reactions Estimated Using Marcus-Hush Theory[a]

reaction	ΔE	ΔE_{pre}	ΔE_{suc}	$\Delta E_0^{\ddagger}$	E_a	$E_a - \Delta E_{pre}$
(1) HFeOH + CCl_4 → HFeClOH + $^{\bullet}CCl_3$	1.3	−2.1	−4.4	17.9[b]	14.9	17.0
(2) $FeCl_2$ + CCl_4 → $FeCl_3$ + $^{\bullet}CCl_3$	10.0	−4.5	−7.7	17.5[b]	16.6	21.1
(3) $^{\bullet}CCl_3$ + CCl_4 → CCl_4 + $^{\bullet}CCl_3$	0	−0.8	−0.8	19.4	18.6	19.4
(4) $FeCl_2$ + $FeCl_3$ → $FeCl_3$ + $FeCl_2$	0	−2.5	−2.5	15.6	13.1	15.6
(5) HFeOH + HFeClOH → HFeClOH + HFeOH	0	−1.0	−1.0	16.5	15.5	16.5

[a] E is the reaction energy; ΔE_{pre} and ΔE_{suc} are the binding energies of precursor and successor complexes, respectively; $\Delta E_0^{\ddagger}$ is the intrinsic barrier, and E_a is the activation energy. [b] Intrinsic barrier taken as the average value of the intrinsic barriers for the component self-exchange reactions.

to the Fe−Cl distances of ∼2.20 Å in the $FeCl_2$ and $FeCl_3$ fragments. In $FeCl_3$, the F−Cl bonds are 2.16 Å, and in $FeCl_2$, they are 2.2 Å. In the $FeCl_2$ moiety of the long-range complex, the Cl−Fe−Cl angle was found to be 163.0°, significantly distorted from the linear conformation of an isolated ground-state $FeCl_2$, while distortions in the $FeCl_3$ moiety were small. The large-angle distortion in the $FeCl_2$ moiety is indicative of a significant charge transfer in the precursor complex. For the quasi-diabatic description of the self-exchange reaction, we constructed a linearly interpolated (in internal coordinates) reaction path (a linear synchronous transit LST[44] pathway) between the starting complex structure $Cl_2Fe\cdots Cl-FeCl_2$ (state A, Figure 1) and the successor complex $Cl_2Fe-Cl\cdots FeCl_2$ (state B, Figure 1). UHF and CCSD(T) energies were calculated at the various interpolated points while maintaining the ($d^5 \times d^6$) electronic structure character on one hand and the ($d^6 \times d^5$) electronic structure character on the other hand. In effect, we determined the quasi-diabatic states and energies corresponding to Cl atom transfer in this system. Considering the strongly ionic character of Fe−Cl bonds, one could view the reactive process as chloride ion Cl^- transfer concerted with electron transfer, the two transfers going in opposite directions, from one Fe to the other. Nonetheless the quasi-diabatic wave functions had the ($d^6 \times d^5$) character and the reverse ($d^5 \times d^6$) character. The midpoint structure was the crossing point structure of the two quasi-diabatic states for Cl atom transfer with Fe−Cl and Cl−Fe distances of 2.56 Å and Cl−Fe−Cl angles of 143.2°.

At the CCSD(T) level, the diabatic crossing point energy was 16.1 kcal/mol relative to the precursor complex. The ground-state/excited-state energy difference calculated with EOM-CCSD(T) was 1.0 kcal/mol. Thus, we estimate the barrier for the self-exchange reaction 4 to be 0.5 kcal/mol lower than the adiabatic crossing point, or 15.6 kcal/mol. The precursor complex is 2.5 kcal/mol more stable than the separated reactants. The Fe−Cl bond-dissociation energy for $FeCl_3$ is 52.0 kcal/mol.

HFeOH + HFeClOH Cl Exchange Reaction 5. We followed the same approach to estimate the barrier to reaction 5 for Cl exchange in HFeOH/HFeClOH as we did for the $FeCl_2/FeCl_3$ self-exchange reaction. As with $FeCl_2/FeCl_3$, DFT was unsuccessful in yielding a stable minimum on the PES. The optimization of the precursor complex was done in C_s symmetry, and a collinear exchange was forced by constraining the Fe−Cl−Fe angle to 180°. As mentioned earlier, this was done to prevent OH and Cl from bridging the Fe centers. In the optimized complex, the Fe−Cl bond distances are 2.22 and 2.95 Å. As the Cl atom is transferred between the two moieties, the H−Fe−O angle opens up from 124.1° in the HFeClOH fragment to 165.2°. The OH groups are in a trans orientation relative to the Fe−Cl−Fe bond, and other bonds and angles change only slightly. The zero-point corrected CCSD(T) barrier at the crossing point is +17.2 kcal/mol relative to the precursor complex energy. The energy splitting between the ground and excited adiabatic states calculated with EOM-CCSD(T) is 1.4 kcal/mol, yielding an adiabatic barrier of 16.5 kcal/mol. The energy of the precursor complex is 1.0 kcal/mol lower than the energy of the separated reactants. The Fe−Cl bond dissociation energy for HFeOHCl is 60.7 kcal/mol.

Estimation of Barriers Using Marcus−Hush Theory. Here, we use the data reported above to estimate the barriers for reactions 1 and 2 following Marcus−Hush theory. Because the atom-dropping experiments were carried in the temperature range of 35−150 K and because ΔG approaches ΔE for $T \rightarrow 0$ K, we approximate the free energy in eq 6 with zero-point corrected electronic energies (eq 7) as indicated earlier.

$$E_a = \Delta E_{pre} + \Delta E_0^{\ddagger}\left(1 + \frac{\Delta E - \Delta E_{pre} + \Delta E_{suc}}{4\Delta E_0^{\ddagger}}\right)^2 \quad (7)$$

Thus, Table 1 shows the reaction energies ΔE, the binding energies of encounter (precursor and successor) complexes ΔE_{pre} and ΔE_{suc}, the intrinsic barriers $\Delta E_0^{\ddagger}$, and the resulting activation barriers E_a.

For reaction 1, we obtain an intrinsic barrier of $\Delta E_0^{\ddagger}$ = 17.9 kcal/mol and E_a = 14.9 kcal/mol for the separated reactants. Relative to the precursor complex, the barrier is 17.0 kcal/mol. This estimate of the barrier is lower than the barrier of 23.8 kcal/mol estimated from the crossing point in Figure 2. The discrepancy between these two values may be due to the approximate nature of the Marcus−Hash approach. Alternatively, our analysis of diabatic states that cross in Figure 2 may overestimate the barrier because we used geometries on the DFT IRC. Regardless of which approach we consider, the barrier estimates are sufficiently high to preclude reaction in the atom-dropping experiments.

For reaction 2, we calculated the reaction endothermicity from separated reactants to separated products to be ∼10 kcal/mol. The precursor complex was found to be 4.5 kcal/mol more stable than the separated reactants, and the successor complex was 7.7 kcal/mol more stable than the separated products. We found a second successor complex (Figure 3), which exhibited an Fe−C bond. This complex was ∼1.4 kcal/mol more stable than the separated reactants CCl_4 + $FeCl_2$. Using the Marcus−Hush cross relationship to characterize the barrier to reaction 2, we found the cross reaction to have a high barrier because both self-exchange reactions were estimated to have high barriers. From the reactions 2 and 3 in Table 1, we estimated the intrinsic barrier to the $FeCl_2$ + CCl_4 to be 17.5 kcal/mol. The successor complex $FeCl_3\cdots CCl_3$ was 6.8 kcal/mol higher in energy than the precursor complex, and the overall reaction was 10 kcal/mol endothermic. Thus, the activation barrier for $FeCl_2/CCl_4$ reaction is higher than the intrinsic barrier; it is 21.1 kcal/mol relative

to the precursor complex and 16.6 kcal/mol relative to the separated reactants. This estimate is in agreement with the estimate of Parkinson et al.[6] that the barrier for surface reactions of CCl_4 with $FeCl_2$ must be larger than ~12 kcal/mol. Our result is also consistent with the barriers determined by Cornia et al.[9] for the reactions of $FeCl_2$ + Cl_3C-R in acetonitrile.

CONCLUSION

We investigate the title reactions to gain insight into the absence of reactivity of HFeOH and $FeCl_2$ toward CCl_4 in atom-dropping experiments.[2,3] The reaction of HFeOH with CCl_4 is calculated to be practically thermoneutral, and the reaction of $FeCl_2$ with CCl_4 is endothermic, although follow-up reactions between $^{\bullet}CCl_3$ and Fe^{III} intermediates leading to the formation of Fe−C bonded complexes are exothermic. The electronic structure description of the reaction paths invokes unpairing two electrons in the d shell of the Fe^{II} system and recoupling these electrons with two electrons from a C−Cl bond of CCl_4. At the crossing point, the C−Cl bond is significantly stretched, and the Fe−Cl bond is partially formed. Thus, the reaction may be characterized as atom transfer or inner-sphere electron transfer in which the C−Cl scission is concerted with electron transfer. The mechanism differs from that often invoked for electrochemical reduction in which the cleaved Cl^- is stabilized by interaction with $^{\bullet}CCl_3$ and/or solvent.[45] We estimated a barrier for Cl atom transfer from CCl_4 to HFeOH to be ~24 kcal/mol above the energy of the reactant encounter complex using the CCSD(T) level of theory at DFT optimized structures. A Marcus−Hush theory treatment yielded a smaller value (~17.0 kcal/mol), yet sufficiently high to hinder reactivity at low temperatures. We also estimated the energy barrier for Cl transfer in $FeCl_2$ + CCl_4 to be ~21 kcal/mol using Marcus−Hush theory. These results explain the absence of reactivity in atom-dropping experiments involving CCl_4 reacting with either HFeOH or $FeCl_2$,[2,3] the high barriers being due to high intrinsic barriers of the component self reactions and the endothermicities of reactions 1 and 2.

ASSOCIATED CONTENT

Supporting Information. Coordinates of structures, electronic energy frequencies, and zero-point energies are provided. This material is available free of charge via the Internet at http://pubs.acs.org.

AUTHOR INFORMATION

Corresponding Author
*E-mail: donald.camaioni@pnl.gov.

ACKNOWLEDGMENT

The authors acknowledge valuable discussions with our collaborators, Drs. Gareth S. Parkinson, Zdenek Dohnalek, R. Scott Smith, Bruce D. Kay, and Don Baer. This work was supported by the U.S. Department of Energy Office of Basic Energy Sciences, Division of Chemical Sciences, Geosciences, and Biosciences. Pacific Northwest National Laboratory is operated for the U.S. Department of Energy by Battelle under Contract No. DE-AC06-76RLO 1830. This research used resources of the National Energy Research Scientific Computing Center, which is supported by the Office of Science of the U.S. Department of Energy under Contract No. DE-AC02-05CH11231.

REFERENCES

(1) Tratnyek, P. G.; Johnson, R. L. *Nano Today* **2006**, *1*, 44.
(2) Parkinson, G. S.; Dohnálek, Z.; Smith, R. S.; Kay, B. D. *J. Phys. Chem. C* **2010**, *114*, 17136.
(3) Parkinson, G. S.; Dohnálek, Z.; Smith, R. S.; Kay, B. D. *J. Phys. Chem. C* **2009**, *113*, 1818.
(4) Camaioni, D. M.; Ginovska, B.; Dupuis, M. *J. Phys. Chem. C* **2009**, *113*, 1830.
(5) Cho, H.-G.; Lyon, J. T.; Andrews, L. *Organometallics* **2008**, *27*, 5241.
(6) Parkinson, G. S.; Kim, Y. K.; Dohnálek, Z.; Smith, R. S.; Kay, B. D. *J. Phys. Chem. C* **2009**, *113*, 4960.
(7) Asscher, M.; Vofsi, D. *J. Chem. Soc. B* **1968**, 947.
(8) Wilputte-Steinert, L. *Transition Met. Chem.* **1978**, *3*, 172.
(9) Cornia, A.; Folli, U.; Sbardellati, S.; Taddei, F. *J. Chem. Soc., Perkin Trans. 2* **1993**, 1847.
(10) Mebel, A. M.; Hwang, D. Y. *J. Phys. Chem. A* **2001**, *105*, 7460.
(11) Zhang, L.; Zhou, M.; Shao, L.; Wang, W.; Fan, K.; Qin, Q. *J. Phys. Chem. A* **2001**, *105*, 6998–7003.
(12) Gutsev, G. L.; Mochena, M. D.; Bauschlicher, C. W., Jr. *Chem. Phys.* **2005**, *314*, 291.
(13) Marcus, R. A.; Sutin, N. *Biochim. Biophys. Acta* **1985**, *811*, 265.
(14) (a) Marcus, R. A. *Annu. Rev. Phys. Chem.* **1964**, *15*, 155. (b) Marcus, R. A. *J. Chem. Phys.* **1965**, *43*, 679.
(15) Hush, N. *Trans. Faraday Soc.* **1961**, *57*, 557.
(16) Blowers, P.; Masel, R. I. *J. Phys. Chem. A* **1999**, *103*, 7047.
(17) (a) Marcus, R. A. *J. Phys. Chem.* **1968**, *72*, 891. (b) Cohen, A. O.; Marcus, R. A. *J. Phys. Chem.* **1968**, *72*, 4249.
(18) (a) Mayer, J. M. *Acc. Chem. Res.* **2010**, *44*, 36. (b) Warren, J. J.; Mayer, J. M. *Proc. Natl. Acad. Sci. U.S.A.* **2010**, *107*, 5282.
(19) Schwarz, C. L.; Bullock, R. M.; Creutz, C. *J. Am. Chem. Soc.* **1991**, *113*, 1225.
(20) Schwarz, C. L.; Endicott, J. F. *Inorg. Chem.* **1995**, *34*, 4572.
(21) Smith, T. P.; Iverson, D. J.; Droege, M. W.; Kwan, K. S.; Taube, H. *Inorg. Chem.* **1987**, *26*, 2882.
(22) (a) Farazdel, A.; Dupuis, M. *J. Comput. Chem.* **1990**, *12*, 276. (b) Farazdel, A.; Dupuis, M.; Clementi, E.; Aviram., A. *J. Am. Chem. Soc.* **1990**, *112*, 4206.
(23) Hirata, S.; Fan, P.-D.; Auer, A. A.; Nooijen, M.; Piecuch, P. *J. Chem. Phys.* **2004**, *121*, 12197.
(24) Kowalski, K.; Hirata, S.; łoch, M. W.; Piecuch, P.; Windus, T. L. *J. Chem. Phys.* **2005**, *123*, 074319.
(25) Stanton, J. F.; Bartlett, R. J. *J. Chem. Phys.* **1993**, *98*, 7029–7039.
(26) Frisch, M. J.; et al. *Gaussian 98*; Gaussian, Inc.: Pittsburgh, PA, 1998.
(27) Frisch, M. J.; et al. *Gaussian 09*, revision A.01; Gaussian, Inc.: Pittsburgh, PA, 2009.
(28) (a) Bylaska, E. J.; et al. *NWChem*, A Computational Chemistry Package for Parallel Computers, version 5.1.1; Pacific Northwest National Laboratory: Richland, WA, 2009. (b) Kendall, R. A.; Aprà, E.; Bernholdt, D. E.; Bylaska, E. J.; Dupuis, M.; Fann, G. I.; Harrison, R. J.; Ju, J.; Nichols, J. A.; Nieplocha, J.; Straatsma, T. P.; Windus, T. L.; Wong, A. T. High Performance Computational Chemistry: An Overview of NWChem a Distributed Parallel Application. *Comput. Phys. Commun.* **2000**, *128*, 260.
(29) Hohenberg, P.; Kohn, W. *Phys. Rev.* **1964**, *136*, B864.
(30) Kohn, W.; Sham, L. *J. Phys. Rev.* **1965**, *140*, A1133.
(31) (a) Rassolov, V.; Pople, J. A.; Ratner, M.; Windus, T. L. *J. Chem. Phys.* **1998**, *109*, 1223. (b) Francl, M. M.; Petro, W. J.; Hehre, W. J.; Binkley, J. S.; Gordon, M. S.; DeFrees, D. J.; Pople, J. A. *J. Chem. Phys.* **1982**, *77*, 3654. (c) Hehre, W. J.; Ditchfield, R.; Pople, J. A. *J. Chem. Phys.* **1972**, *56*, 2257.
(32) Schafer, A.; Horn, H.; Ahlrichs, R. *J. Chem. Phys.* **1992**, *97*, 2571.
(33) Becke, A. D. *J. Chem. Phys.* **1993**, *98*, 5648.
(34) Schafer, A.; Huber, C.; Ahlrichs, R. *J. Chem. Phys.* **1994**, *100*, 5829.
(35) Seeger, R.; Pople, J. A. *J. Chem. Phys.* **1977**, *66*, 3045.

(36) Bauernschmitt, R.; Ahlrichs, R. *J. Chem. Phys.* **1996**, *104*, 9047.
(37) Watts, J. D.; Dupuis, M. *Mol. Phys.* **2005**, *103*, 2223.
(38) Dobbs, K. D.; Dixon, D. A. *J. Phys. Chem.* **1994**, *98*, 12584.
(39) Zhao, Y.; Truhlar, D. G. *Acc. Chem. Res.* **2008**, *41*, 157.
(40) Zhao, Y.; González-García, N.; Truhlar, D. G. *J. Phys. Chem. A* **2005**, *109*, 2012.
(41) Hammond, G. S. *J. Am. Chem. Soc.* **1955**, *77*, 334.
(42) Krylov, A. I. *J. Phys. Chem.* **2000**, *113*, 6052.
(43) (a) Carpenter, J. E.; Weinhold, F. *J. Mol. Struct.: THEOCHEM* **1988**, *169*, 41. (b) Glendening, E. D.; Reed, A. E.; Carpenter, J. E.; Weinhold. F. *NBO*, version 3.1; Theoretical Chemistry Institute and Department of Chemistry, University of Wisconsin: Madison, Wisconsin.
(44) Halgren, T. A.; Lipscomb, W. N. *Chem. Phys. Lett.* **1977**, *49*, 225.
(45) (a) Pause, L.; Robert, M.; Savéant, J.-M. *J. Am. Chem. Soc.* **2000**, *122*, 9829. (b) Pause, L.; Robert, M.; Savéant, J.-M. *J. Am. Chem. Soc.* **2001**, *123*, 11908. (c) Houmam, A. *Chem. Rev.* **2008**, *108*, 2180.